Article

TRANSPARENT PROCESS OPEN ACCESS

THE EMBO JOURNAL

c-Src drives intestinal regeneration and transformation

Julia B Cordero[1,†], Rachel A Ridgway[1], Nicola Valeri[2], Colin Nixon[1], Margaret C Frame[4], William J Muller[3], Marcos Vidal[1] & Owen J Sansom[1,*]

Abstract

The non-receptor tyrosine kinase c-Src, hereafter referred to as Src, is overexpressed or activated in multiple human malignancies. There has been much speculation about the functional role of Src in colorectal cancer (CRC), with Src amplification and potential activating mutations in up to 20% of the human tumours, although this has never been addressed due to multiple redundant family members. Here, we have used the adult *Drosophila* and mouse intestinal epithelium as paradigms to define a role for Src during tissue homeostasis, damage-induced regeneration and hyperplasia. Through genetic gain and loss of function experiments, we demonstrate that Src is necessary and sufficient to drive intestinal stem cell (ISC) proliferation during tissue self-renewal, regeneration and tumourigenesis. Surprisingly, Src plays a non-redundant role in the mouse intestine, which cannot be substituted by the other family kinases Fyn and Yes. Mechanistically, we show that Src drives ISC proliferation through upregulation of EGFR and activation of Ras/MAPK and Stat3 signalling. Therefore, we demonstrate a novel essential role for Src in intestinal stem/progenitor cell proliferation and tumourigenesis initiation *in vivo*.

Keywords Apc; intestinal stem cells; regeneration; Src; tumourigenesis
Subject Categories Cancer; Signal Transduction; Stem Cells
DOI 10.1002/embj.201387454 | Received 19 November 2013 | Revised 11 March 2014 | Accepted 8 April 2014

Introduction

Since its discovery in the 1970s, the non-receptor tyrosine kinase Src has been implicated in multiple types of human cancers (Irby & Yeatman, 2000). There is rationale for a driver role for Src within CRC, and putative Src activating mutations were reported specifically within CRC, with amplification found in up to 20% of the advanced human CRC tumours (Irby *et al*, 1999; The Cancer Genome Atlas Network, 2012; www.cbioportal.org/public-portal). There is also increased Src activity in progressive stages of CRC (Talamonti *et al*, 1993; Termuhlen *et al*, 1993; Jones *et al*, 2002). Consistent with this, multiple studies have shown high percentage Src activation in CRC and suggested that this upregulation and/or hyperactivation of Src contributes to CRC progression and metastasis (Yeatman, 2004). Studies using Src family kinases (SFKs) inhibitors within CRC cell lines have predominantly shown an impact on invasion rather than proliferation (Serrels *et al*, 2006). One of the difficulties in interpreting the results with SFK inhibitors is the broad number of targets they inhibit. Given the strong evidence for a role for Src in CRC, it is somewhat surprising that Src inhibitors do not inhibit tumour cell proliferation. Therefore, we here performed genetic studies to more definitely address Src's role in the intestine.

CRC is one of the most common cancers and the third most common cause of cancer deaths in the western world. Inactivating mutations in the gene encoding for the negative regulator of Wnt signalling, adenomatous polyposis coli (*Apc*), are detected in 80% of hereditary and sporadic forms of CRC (Kinzler *et al*, 1991; Korinek *et al*, 1997). Mouse models have shown that inactivation of *Apc* is sufficient to drive intestinal hyperplasia (Sansom *et al*, 2004; Andreu *et al*, 2005). Moreover, *Apc* deletion within the murine intestinal stem cells (ISCs) results in rapid adenoma formation suggesting they can act as cells of origin in CRC (Barker *et al*, 2009). Wnt signalling is also required during intestinal regeneration, and this process mimics many of the features of *Apc* loss, further suggesting that stem cell proliferation, for example during regeneration, and cancer initiation are linked and co-regulated by key signalling molecules (Cordero & Sansom, 2012; Cordero *et al*, 2012a,b).

The adult *Drosophila* midgut resembles the vertebrate intestine (Casali & Batlle, 2009), and it has proven to be an extremely useful model to study intestinal homeostasis, regeneration and disease (Biteau *et al*, 2011; Jiang & Edgar, 2012; Seton-Rogers, 2013). The fly intestinal epithelium is self-renewed by dedicated ISCs

1 The Beatson Institute for Cancer Research, Bearsden, Glasgow, UK
2 Institute of Cancer Research, Sutton, London, UK
3 Goodman Cancer Research Center, McGill University, Montreal, QC, Canada
4 Edinburgh Cancer Research Centre, Institute of Genetics & Molecular Medicine, University of Edinburgh, Edinburgh, UK
*Corresponding author: Tel: +44 141 330 3953; E-mail: o.sansom@beatson.gla.ac.uk
†Present address: Wolfson Wohl Cancer Research Centre, Institute of Cancer Sciences, University of Glasgow, Garscube Estate, Switchback Road, Bearsden, Glasgow, UK

(Micchelli & Perrimon, 2006; Ohlstein & Spradling, 2006). Upon division, ISCs give rise to an undifferentiated progenitor, the enteroblast (EB), which differentiate into either the secretory cell linage, enteroendocrine cells (ee) or the absorptive epithelial cell linage represented by the enterocytes (EC). Importantly, recent work from ourselves and others demonstrated that loss of *Apc* from the fly midgut results in ISC hyperproliferation (Lee *et al*, 2009; Cordero *et al*, 2012a) and recapitulates several hallmarks from mouse models and human CRC (Sansom *et al*, 2004, 2007; Cordero *et al*, 2012a).

Unlike the nine SFKs encoded in mammalian genomes, there are only two Src family kinase members in *Drosophila*, Src42A and Src64B as well as a single fly orthologue of the mammalian Src inhibitor, COOH-terminal Src kinase (Csk) and its paralogue, the C-terminal Src kinase homologous kinase (Chk). Hyperactivation of Src in developing *Drosophila* tissues leads to a wide range of outcomes including cell migration, perturbed differentiation, hyperproliferation and apoptosis (Vidal *et al*, 2006, 2007). Indeed, the precise level of Src deregulation is very important to the phenotypic outcome, as the relative levels of Src overexpression compared to surrounding normal cells are vital for *Drosophila* development and mammalian cells in culture (Vidal *et al*, 2007; Kajita *et al*, 2010). However, the mechanism of action of Src in *Drosophila* and mammals *in vivo* is still poorly understood, particularly how it contributes to intestinal homeostasis.

Here, we use *Drosophila* and mouse genetic models to directly address the role of Src within the intestinal epithelium. We show that Src is necessary and sufficient to drive ISC proliferation during normal tissue homeostasis, damage-induced regeneration and tumour development *in vivo*. We define, for the first time, key roles for EGFR/Ras/MAPK and Stat signalling as functional mediators of Src-dependent ISC proliferation.

Results

Ectopic Src activation is observed in mouse models of CRC

Src is either hyperactivated or amplified in human CRCs (Yeatman, 2004). We tested whether this was also the case in the mouse intestine. We stained tissue sections from mouse small intestines with an antibody to detect the activated form of Src (pSrc), which cross-reacts with other p-SFKs (Fig 1A–D). Intestines from control animals showed membrane pSrc staining, which was largely restricted to the proliferative 'crypt' region of the intestinal epithelium (Fig 1A). No pSrc staining was observed in tissues form mice bearing conditional depletion of *Src* from the intestinal epithelium combined with constitutive loss of related kinases Fyn and Yes (*AhCre* $Src^{fl/fl}$; $Fyn^{-/-}$; $Yes^{-/-}$; Fig 1B). These results confirm the specificity of the antibody to pSFKs in the mouse intestine and indicate that Src, Fyn and Yes are the major SFKs expressed in this tissue. We next analysed the pSrc levels in mouse models of CRC. While we observed no change in *Src* transcription (data not shown), pSrc immunoreactivity was significantly expanded throughout the hyperproliferative 'crypt progenitor cell-like' domain of the intestinal epithelium from mice subject to acute loss of *Apc* (Fig 1C, dotted line; Sansom *et al*, 2004). Similarly, ectopic pSrc staining was observed within the core of intestinal polyps from $Apc^{Min/+}$ mice (100%; $n = 10$; Fig 1D). To visualize Src activation at the early stages of human CRC, we stained non-invasive human adenomas for pSrc and found it consistently upregulated (100%; $n = 7$; Fig 1E and F). Therefore, ectopic activation of SFK is detected from the earliest stages of transformation following *Apc* loss, prior to the formation of invasive tumours and dissemination. This suggested that SFKs might have important roles in the initial stages of tumourigenesis in addition to their recognized roles in invasion and metastasis (Yeatman, 2004).

Src overexpression is sufficient to drive intestinal hyperproliferation

We next asked whether elevated SFK activity was a driver of intestinal hyperproliferation, or a passive event. To address this, we used the adult intestine of *Drosophila melanogaster*, which was previously validated as a model system to study aspects of CRC (Cordero *et al*, 2009, 2012a; Lee *et al*, 2009). Unlike the mouse intestine, which contains proliferating stem- and transit-amplifying (TA) cells, only the stem cells are proliferative in the adult *Drosophila* midgut (Micchelli & Perrimon, 2006; Ohlstein & Spradling, 2006). Therefore, assessment of mitotic proliferation in the fly midgut represents a direct measure of ISC proliferation. We used the temperature-sensitive driver *escargot-gal4, UAS-GFP; tubulin-gal80*^{ts} ($esg^{ts} > gfp$; Micchelli & Perrimon, 2006) to induce overexpression of Src within ISCs/EBs (stem/progenitor cells) in the adult *Drosophila* midgut. The ectopic activation of Src kinase was achieved by overexpression of independent *UAS-Src* transgenes—wild-type *Src64B* ($esg^{ts} > Src64^{WT}$) and constitutively active form of *Src42A* ($esg^{ts} > Src42^{CA}$)—or by overexpression of an RNA interference transgene to knockdown Csk (Vidal *et al*, 2006; $esg^{ts} > Csk\text{-}IR$). All three approaches resulted in substantial ISC hyperproliferation and hyperplasia of the adult *Drosophila* intestine (Fig 1G and H and Supplementary Fig S1). Histological analysis of sections of paraffin-embedded midguts from 7-day-old $esg^{ts} > Src64^{WT}$ animals revealed 'polyp-like' structures containing multiple big and small $BrdU^{+ve}$ cell nuclei, which were not observed in age-matched control intestines (Fig 1I and I' and Supplementary Fig S1A and B). To further characterize the phenotype of $esg^{ts} > Src64^{WT}$ midguts, we stained tissues with anti-pH3 (Fig 1J–K') and anti-Delta (Fig 1M–O) antibodies to specifically label cells undergoing active mitosis and ISCs, respectively. Src–overexpressing midguts showed significant upregulation in the number of $pH3^{+ve}$ and $Delta^{+ve}$ cells when compared with control counterparts (Fig 1J–P and Supplementary Fig S1C and C'). Consistent with previous reports (Micchelli & Perrimon, 2006; Ohlstein & Spradling, 2006), $pH3^{+ve}$ staining was restricted to small nuclei ISCs (Fig 1J–K') indicating that big $BrdU^{+ve}$ cell nuclei (Fig 1I') are likely to represent newly made, endoreplicating enterocytes (ECs; Micchelli & Perrimon, 2006). Importantly, Src-dependent ISC hyperproliferation in the midgut was largely suppressed by concomitant overexpression of the human homologue of Csk, Chk (Vidal *et al*, 2006; Fig 1L and Supplementary Fig S1G–J), highlighting the conserved nature of SFK regulation by upstream inactivating kinases. Altogether, these data demonstrate that enhanced expression of Src in stem/progenitor cells is sufficient to drive hyperproliferation and increase numbers of ISCs in the adult *Drosophila* midgut.

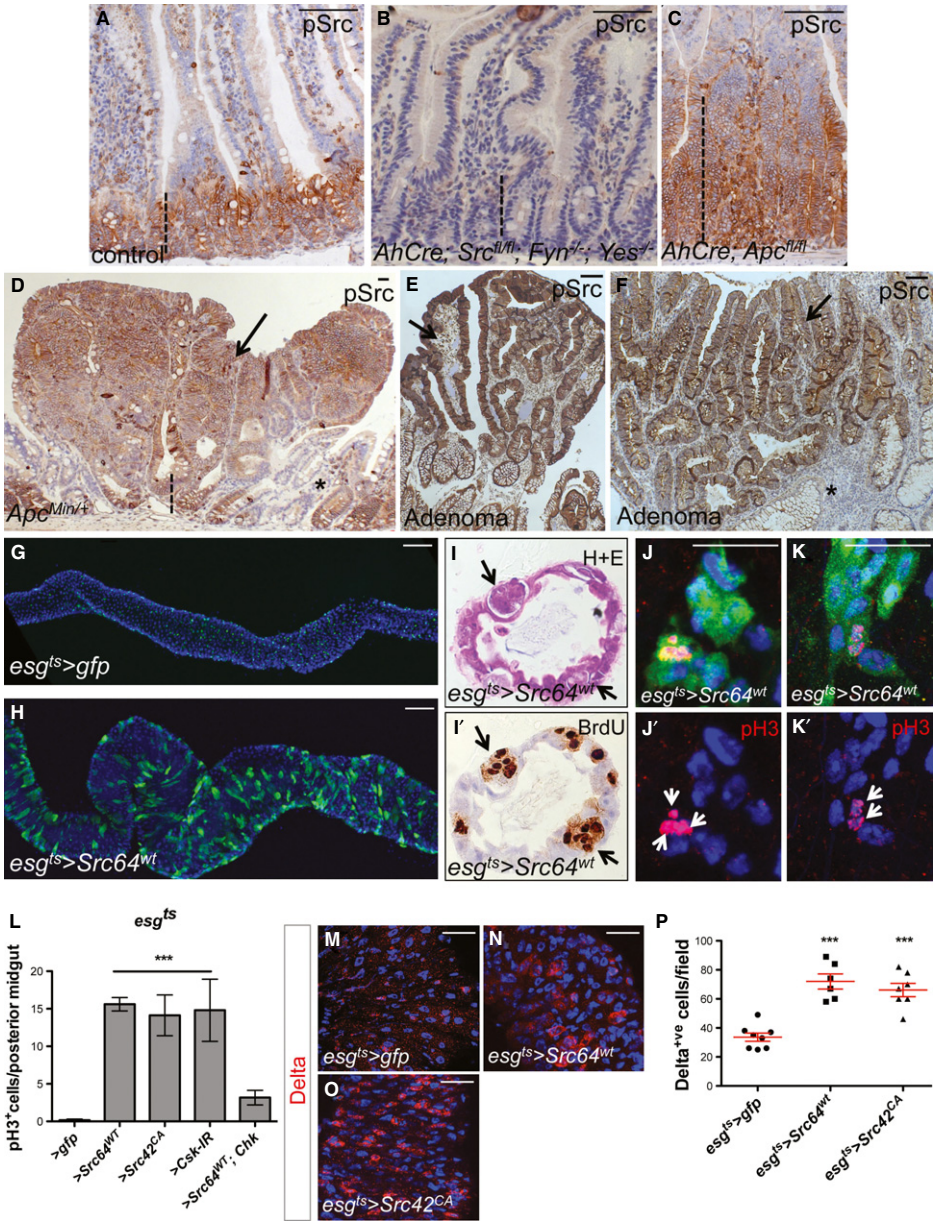

Figure 1. Src upregulation drives ISC proliferation.

A–D Immunohistochemistry to detect the activated form of Src (pSrc) in tissue sections from mouse and human intestines. pSrc is detected in the proliferative 'crypt' region (indicated with dashed line) at the base of the mouse small intestinal epithelium in control animals (A). Conditional knockout of *Src* ($Src^{fl/fl}$) combined with full knockout of related kinases *Fyn* and *Yes*, resulted in no staining within the intestinal epithelium (B). Intestines with conditional *Apc* knockout ($Apc^{fl/fl}$) depict the expected 'crypt-like' progenitor phenotype (dashed line) and expansion of the pSrc domain (C). Example of a small intestinal polyp from an $Apc^{Min/+}$ mouse, showing high p-Src staining within the core of the polyp (arrow), is shown in (D). Note normal tissue around polyp showing pSrc localized at the crypt base (dashed line). Scale bars, 100 μm.

E, F pSrc is upregulated within benign human intestinal adenoma lesions (arrows) when compared with normal surrounding tissue (asterisks). Scale bars, 100 μm.

G, H Adult *Drosophila* midguts overexpressing *gfp* (G; control) or *Src* (H) for 7 days under the stem/progenitor cell (ISCs/EBs) driver *escargot-gal4* ($esg^{ts} > gfp$ and $esg^{ts} > Src64^{wt}$, respectively). Unless otherwise noted green marks *esg* > *gfp* cells and Dapi (blue) stains all cell nuclei. Scale bars, 100 μm.

I, I' Paraffin-embedded sections from 7-day-old Src-overexpressing midguts ($esg^{ts} > Src64^{wt}$) analysed by Haematoxylin and Eosin H+E (I) and BrdU (I') staining. Arrows point to 'polyp-like' structures containing $BrdU^{+ve}$ cells.

J–K' 7-day-old $esg^{ts} > Src64^{wt}$ posterior midguts stained with anti-pH3 (red) to visualize proliferating ISCs (arrows). Scale bars, 20 μm.

L ISC proliferation quantified as the number of cells which stained positive for phosphorylated histone 3 (pH3) in posterior midguts from control animals ($esg^{ts} > gfp$) or animals overexpressing *Src* ($esg^{ts} > Scr64^{wt}$ or $esg^{ts} > Src42^{CA}$) or RNA interference for the Src inhibitor Csk ($esg^{ts} > Csk\text{-}IR$). Note that co-expression of human ChK ($esg^{ts} > Scr64^{wt}$; *Chk*) suppresses Src-driven hyperproliferation in the *Drosophila* midgut.

M–O 7-day-old adult posterior midguts from animals of the indicated genotypes stained with anti-Delta (red) to label ISCs. Scale bars, 20 μm.

P Quantification of the number of $Delta^{+ve}$ ISCs per field from posterior midguts as in (M-O).

Data information: Data in (L) and (P) represent average values ± SEM (***$P < 0.0001$ one-way ANOVA with Bonferroni's multiple comparison test)

Src is required to drive stem cell proliferation during intestinal homeostasis and regeneration

We next tested whether endogenous Src was required for proliferation within the *Drosophila* intestine. To do this, we examined the role of Src in homeostatic self-renewal and damage-induced regeneration of the adult midgut.

Like its vertebrate counterpart, the adult *Drosophila* posterior midgut is replenished by dedicated ISCs and displays a remarkable regenerative response to damaging agents (Cordero & Sansom, 2012). Damage-induced intestinal regeneration is characterized by an acute expansion of the stem/progenitor cell population and increase in ISC proliferation, which is required to regenerate the damaged intestinal epithleium (Amcheslavsky *et al*, 2009; Buchon *et al*, 2009; Jiang *et al*, 2009; Fig 2A and B). We first assessed the regulation of Src during intestinal regeneration after feeding flies with the pathogenic bacteria *Pseudomonas entomophila* (*Pe*; Buchon *et al*, 2009; Fig 2A–C). While immunostaining for pSrc showed barely detectable signal in the midgut epithelium from unchallenged animals, pSrc levels became more evident within the intestinal epithelium of animals subject to damage by *Pe* (Fig 2A–B'). RT–qPCR from whole midguts confirmed a threefold transcriptional upregulation of *Src42* in regenerating tissues (Fig 2C). We next tested the functional role of Src42 during intestinal regeneration. We used RNAi transgenes to knockdown *Src42* within stem/progenitors cells of the adult midgut ($esg^{ts} > Src42\text{-}IR$). Knockdown of *Src42* by using two independent RNAi lines resulted in almost complete suppression of ISC proliferation in regenerating midguts (Fig 2D–F and Supplementary Fig S2). Midguts from animals heterozygous for a loss-of-function allele of *Src42* ($Src42^{K10108}$) also showed significantly impaired regeneration (Fig 2F and Supplementary Fig S2C and C') showing that *Src42* is rate-limiting during regeneration. RNAi knockdown of *Src64* did not significantly affect intestinal regeneration (data not shown).

We also noted that $esg^{ts} > Src42\text{-}IR$ midguts looked 'thinner' than their control counterparts (Fig 2E; compare with Fig 2D and Supplementary Fig S2B; compare with Supplementary Fig S2A), even when unchallenged. We therefore tested whether Src42 was required for ISC proliferation during homeostatic self-renewal of the adult midgut. We first overexpressed a *Src42-IR* transgene within the intestinal epithelium using the inducible 'escargot flip out' system ($esg^{ts}\ F/O > gfp$; Jiang *et al*, 2009), in which every progenitor cell and its new progeny will express Gal4 and *UAS-gfp* in addition to the *UAS-Src42-IR* RNAi transgene. We then visualized the newly produced *esg* cell lineage 7, 14 and 30 days after transgene induction (Fig 2G–L). Knockdown of *Src42* from the epithelium of undamaged midguts impaired homeostatic self-renewal in the adult posterior midgut (Fig 2G–L) as evidenced by the reduced *esg* linage labelling in $esg^{ts}\ F/O > Src42\text{-}IR$ midguts after 14 and 30 days of tracing (Fig 2K and L; compare with Fig 2H and I). We next used the MARCM system (Lee & Luo, 1999) to create adult midgut clones from a control transgene (*MARCM LacZ*; Fig 2M–O) or with *Src42* knockdown (*MARCM Src42-IR*; Fig 2P–R) and follow their growth at 7, 14 and 30 days after clonal induction (ACI). No significant difference was observed in the size of control and *Src42-IR* during the intimal phase of clonal growth (Fig 2M, P and S). However, unlike control clones, 14- and 30-day-old *Src42-IR* clones failed to progressively grow over time and even decreased their size (Fig 2Q–S; compare with 2N, O and S). These results indicate that endogenous Src42 activity is essential to sustain ISC proliferation during homeostatic self-renewal as well as to drive ISCs during regeneration of the adult *Drosophila* midgut.

Src is activated downstream of Wg/Wnt signalling in the adult *Drosophila* midgut

c-Src is hyperactivated in response to *Apc* loss in mouse and human intestinal adenomas (Fig 1C–F). Work from us and others has shown that Wnt/Wg signalling drives ISC hyperproliferation and is required for regeneration of the adult *Drosophila* midgut (Lin *et al*, 2008; Lee *et al*, 2009; Cordero *et al*, 2012a,b). We therefore tested whether Src activation was dependent on Wnt signalling in the midgut. *Src42* mRNA showed a 1.7-fold upregulation in whole midguts from animals homozygous for the *Apc1* null allele $Apc1^{Q8}$ (Ahmed *et al*, 1998; Fig 3A). Immunofluorescence staining revealed pSrc upregulation within stem/progenitor cells from $Apc1^{Q8}$ midguts (Fig 3B–C') and in midguts overexpressing Wg ($esg^{ts} > wg$) or an activated from of β–catenin/Armadillo ($esg^{ts} > arm^{S10}$; Fig 1D–F'). Importantly, upregulation of pSrc upon *Pe* infection was impaired in midguts unable to regenerate due to *wg* knockdown in stem/progenitor cells ($esg^{ts} > wg\text{-}IR$; Fig 3G–I'). Altogether these results suggest that Wnt signalling is necessary and sufficient for Src activation in the *Drosophila* midgut.

Figure 2. Src is required for ISC proliferation during homeostasis and regeneration of the adult *Drosophila* midgut.

A–B' Immunofluorescence staining to detect pSrc (red) in midguts from *esg* > *gfp* (green) animals after feeding with Sucrose (Suc) (A, A') or subject to intestinal damage by feeding bacteria (*Pe*) (B, B'). Arrows point to examples of cell membranes stained with anti-pSrc. Scale bars, 20 μm.

C qRT-PCR from whole midguts as in (A–B') to detect transcript levels of *Drosophila Src42* and *Src64*. Only *Src42* was significantly upregulated in damaged midguts. Data represents average values ± SEM.

D–E' Posterior midguts from 14-day-old Suc- or *Pe*-fed control animals (D, D'; $esg^{ts} > gfp$) or animals subject to RNAi knockdown of *Src42* in ISCs/EBs (E, E'; $esg^{ts} > Src42\text{-}IR$).

F Quantification of ISC proliferation in regenerating posterior midguts from animals of the indicated genotypes and treated as in (D–E'). Data represent average values ± SEM (***$P < 0.0001$ one-way ANOVA with Bonferroni's multiple comparison test).

G–L Homeostatic self-renewal in control and *Src42-IR* posterior midguts using the *escargot* 'flip out' system ($esg^{ts}\ F/O$). The lineage from *gfp* (control) and *Src42-IR* esg^{+ve} cells (green) was analysed 7, 14 and 30 days after transgene induction. Scale bars, 50 μm.

M–R Adult posterior midguts carrying 7-, 14- and 30-day-old MARCM clones (green) from a control transgene (M–O; *LacZ*) or from *Src* RNAi (P–R; *Src42-IR*). Scale bars, 20 μm.

S Quantification of the number of cells per clone in posterior midguts as in (M–R). Note that, unlike their control counterparts, MARCM *Src42-IR* clones failed to grow and even decreased in size over time. Clonal size distribution is presented as a dot plot with the mean clonal size ± SEM (***$P < 0.0001$; **$P < 0.001$ one-way ANOVA with Bonferroni's multiple comparison test).

Src is required for tumourigenesis after Apc loss in *Drosophila*

We next tested the functional role of *Src42* in ISC hyperproliferation driven by loss of *Apc1* in the adult *Drosophila* midgut (Cordero *et al*, 2012a). We created adult midgut clones of cells deficient for *Apc1* only (*MARCM Apc1*^{Q8}; Fig 4B) or combined with *Src42* knockdown (*MARCM Src42-IR; Apc1*^{Q8}; Fig 4D). As previously reported, posterior midgut *Apc1*$^{-/-}$ mutant clones contained significantly more cells and displayed increased ISC proliferation when compared with control (*MARCM Lac-Z*) clones (Cordero *et al*, 2012a; Fig 4A, B, E and F). Consistent with our previous results (Fig 2M–S), *Src42-IR* clones (*MARCM Src42-IR*) were smaller than control clones (Fig 4A, C, E and F). Importantly, knocking down *Src42* inhibited hyperproliferation in *Apc1*$^{-/-}$ clones (Fig 4B, D, E and F). These data demonstrate an essential role for Src42 in Apc1-dependent ISC hyperproliferation in the adult *Drosophila* midgut.

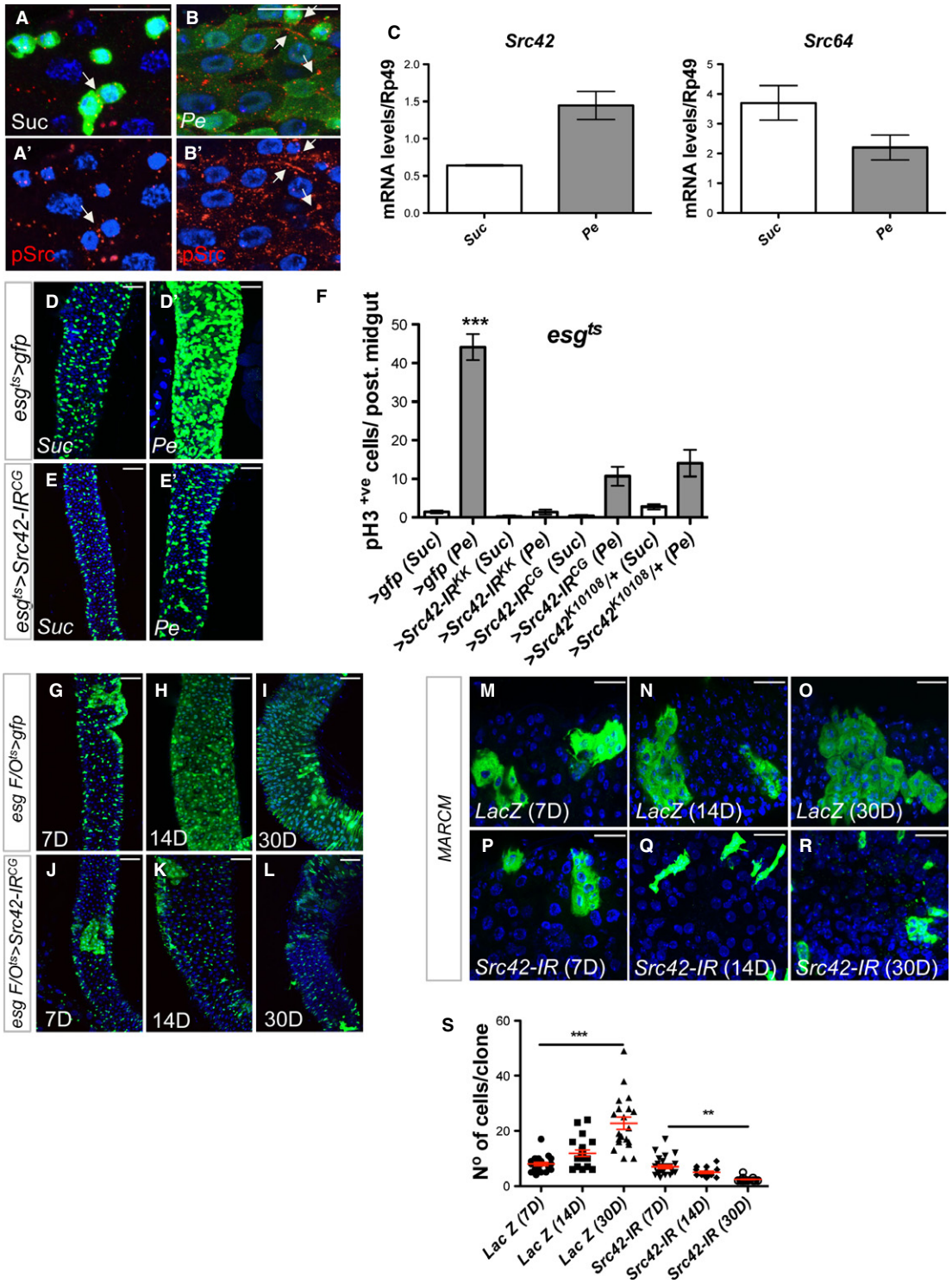

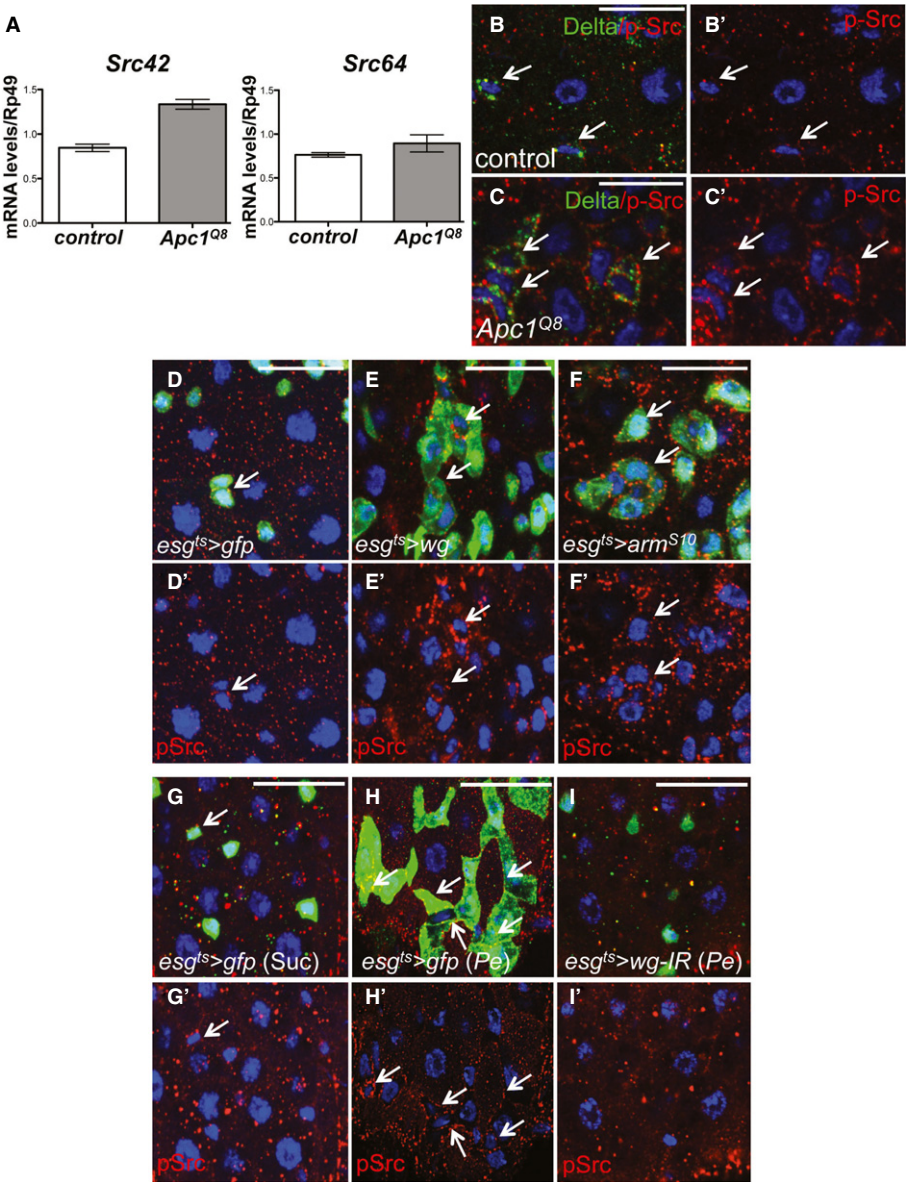

Figure 3. Src is activated downstream of Wnt signalling in the adult *Drosophila* midgut.

A qRT-PCR of whole midguts from 7-day-old control and $Apc1^{-/-}$ ($Apc1^{Q8}$) animals to assess transcript levels of *Src42* and *Src64*. Only *Src42* was significantly upregulated in the midgut in response to *Apc1* loss. Data represent average values ± SEM.

B–C' 7-day-old control (B, B') and $Apc1^{Q8}$ midguts (C, C') co-stained with anti-pSrc (red) and anti-Delta (green). $Apc1^{Q8}$ midguts display significant pSrc upregulation within $Delta^{+ve}$ ISCs (arrows). Scale bars, 20 μm.

D–F' pSrc immunofluorescence (red) in 14-day-old midguts from control animals or animals subjected to Wg signalling upregulation by overexpressing Wg or activated β-catenin/Armadillo within ISCs/EBs ($esg^{ts} > gfp$; $esg^{ts} > wg$ and $esg^{ts} > arm^{S10}$, respectively). Note pSrc upregulation in ISCs/EBs in response to Wg signalling activation (arrows). Scale bars, 20 μm.

G–I' pSrc staining (red) in 14-day-old midguts from control animals or animals subject to *wg* knockdown by overexpressing a *wg* RNAi within ISCs/EBs (esg^{ts}>*wg-IR*) and fed with Suc (G, G') or *Pe* (H-I'). Note that pSrc upregulation in ISCs/EBs upon *Pe* feeding (H, H'; arrows) is suppressed by *wg* knockdown (I, I'). Scale bars, 20 μm.

Src drives ISC hyperproliferation through regulation of the EGFR/MAPK and Stat signalling pathways

The EGFR/Ras/MAPK and Jak/Stat signalling pathways are required for *Drosophila* intestinal homeostasis and regeneration (Buchon *et al*, 2009; Jiang *et al*, 2009, 2011; Beebe *et al*, 2010; Biteau & Jasper, 2011) and are essential mediators of Apc1-driven intestinal hyperproliferation (Cordero *et al*, 2012a). We therefore tested whether these pathways were potential mediators of the role of Src in ISC proliferation *in vivo*. Src overexpression ($esg^{ts} > Src64^{WT}$ and $esg^{ts} > Src42^{CA}$) resulted in ectopic activation of MAPK/Erk1/2 (pErk1/2; Fig 5A, A', C, C', E-G and not shown). Such phenotype resembled the one resulting from overexpression of activated Ras in stem/progenitor cells (Jiang *et al*, 2011) and correlated with

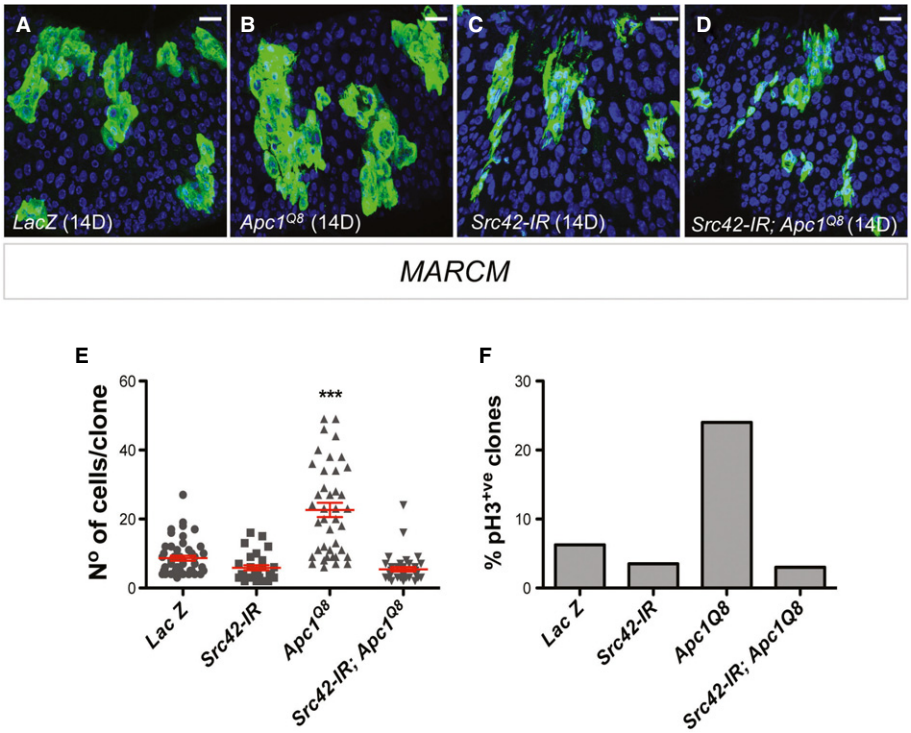

Figure 4. Src mediates Apc1-dependent intestinal hyperproliferation in the *Drosophila* midgut.

A–D Adult posterior midguts carrying 14-day-old MARCM clones (green) of the indicated genotypes. Scale bars, 20 μm.

E, F Quantification of the number of cells per clone (E) and percentage of $pH3^{+ve}$ clones (F) in posterior midguts as in (A–D). Note that *Src42* knockdown completely suppressed ISC proliferation in $Apc1^{Q8}$ MARCM clones (B, D, E, F). Clonal size distribution is presented as a dot plot with the mean clonal size ± SEM (***$P < 0.0001$ one-way ANOVA with Bonferroni's multiple comparison test).

upregulation of total levels of EGFR within the same cells (Fig 5B, B', D and D' and not shown). Transcriptional upregulation of *egfr* by Src overexpression was confirmed through qRT–PCR from whole midguts (Fig 5H). Importantly, knocking down EGFR or Ras completely suppressed ISC hyperproliferation in $esg^{ts} > Src$ midguts (Fig 5J–L and Supplementary Fig S3A-I). Altogether, our results suggest that EGFR expression and downstream pErk activation are key mediators of intestinal hyperproliferation driven by Src.

qRT–PCR of Src-overexpressing midguts also indicated a significant upregulation of the Jak/Stat target *Socs36E* (Fig 5I). To test the functional relevance of Jak/Stat signalling activation in $esg^{ts} > Src$ midguts, we combined *Src* overexpression with RNAi knockdown for *stat92E/marrelle* ($esg^{ts} > stat\text{-}IR; Src42^{CA}$) or the Upd/IL-6 receptor *domeless* ($esg^{ts} > dome\text{-}IR; Src42^{CA}$; Fig 5M). Unlike in intestinal regeneration and Apc1-dependent hyperproliferation (Buchon *et al*, 2009; Jiang *et al*, 2009; Cordero *et al*, 2012a), *Stat* but not *dome* knockdown suppressed Src-dependent ISC hyperproliferation in the adult *Drosophila* midgut (Fig 5M and Supplementary Fig S3J–M). These results support a direct activation of Stat by Src (Yu *et al*, 1995; Cao *et al*, 1996), which does not involve cytokine receptor. Previous work on the *Drosophila* eye imaginal disc links Src-dependent overgrowth to parallel activation of Stat and JNK signalling (Read *et al*, 2004). qRT–PCR to assess levels of the JNK target gene *puckered* (*puc*) shows that Src overexpression results in JNK upregulation in the midgut (Supplementary Fig S3R). However, blocking JNK signalling within stem/progenitor cells does not mediate Src-dependent hyperproliferation in the fly midgut (Supplementary Fig S3S and T). Similar outcomes have been reported in the analysis of JNK activation and requirement during intestinal regeneration in *Drosophila* (Jiang *et al*, 2009). Together these results place EGFR/MAPK and Stat activation as key *in vivo* mediators of Src-driven stem cell hyperproliferation in the *Drosophila* intestine.

Mammalian SFKs are redundant for intestinal homeostasis

An important question posed by our results on the role of Src in the *Drosophila* intestine was whether these would translate to the mammalian system. We first assessed whether there was an exclusive role of Src in the adult mammalian intestine.

Using the 'Cre-Lox' technology (Sauer, 1998), we conditionally knocked out Src from the epithelium of the mouse small intestine. To achieve this, we bred mice carrying a LoxP-flanked *Src* allele ($Src^{fl/fl}$; Marcotte *et al*, 2012) with mice carrying a Cre recombinase driven under the control of the Cyp1A1 aryl hydrocarbon-responsive promoter (*AhCre*). Induction of *AhCre* recombinase results in high penetrance Cre expression within the intestinal epithelium and liver (Ireland *et al*, 2004; Reed *et al*, 2008; Supplementary Fig S5K). Deletion of Src from the mouse intestinal epithelium ($AhCre\ Src^{fl/fl}$; *Src KO*) resulted in no apparent defects in homeostatic self-renewal of unchallenged intestines (Fig 6A and B). We next conditionally knocked out all SFKs expressed in the intestine: Src, Fyn and Yes (Fig 1B; $AhCre\ Src^{fl/fl}\ Fyn^{-/-}\ Yes^{-/-}$; *Src Fyn Yes KO*; Fig 6C). Those

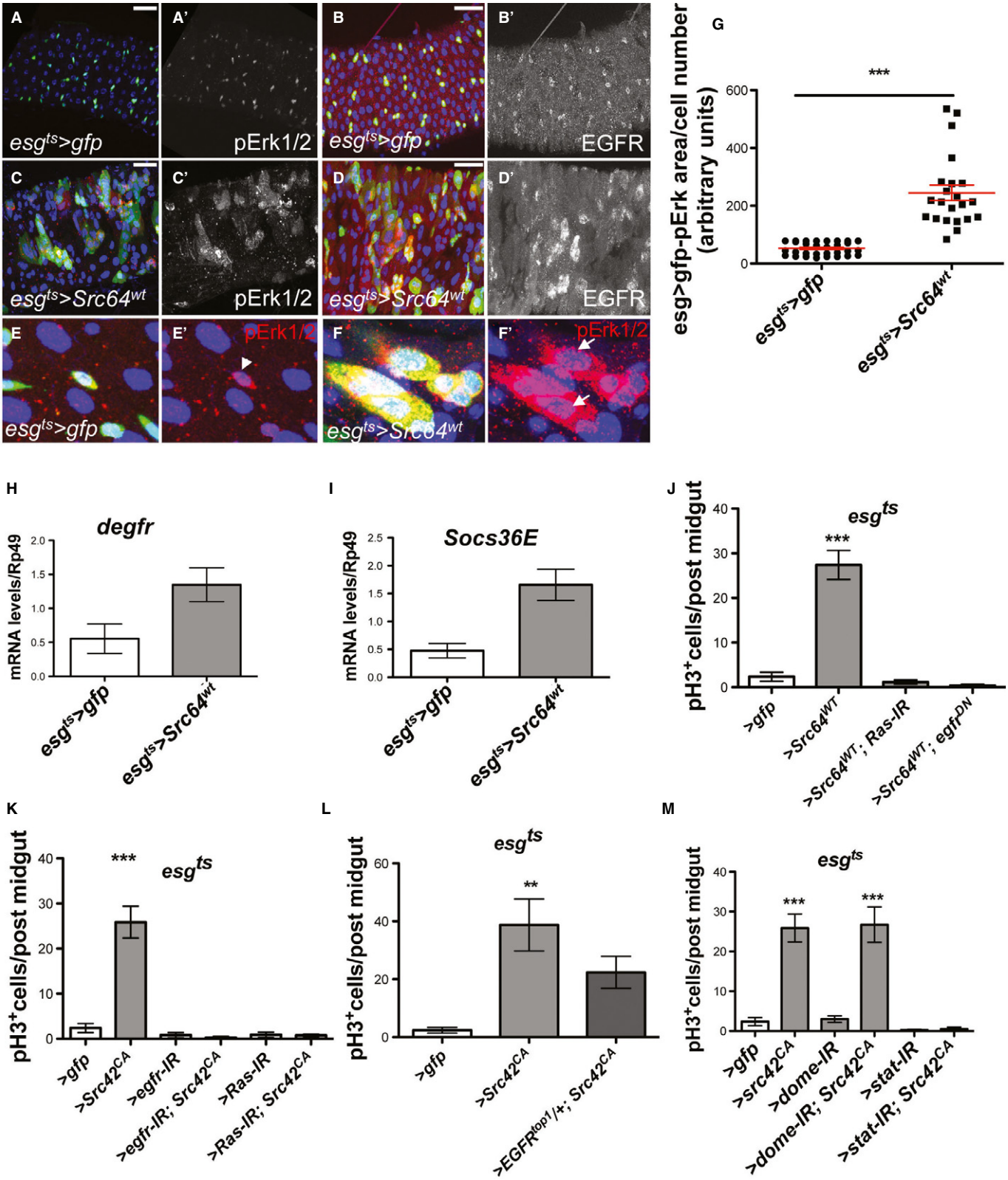

mice displayed multiple signs of poor health 4 days post-Cre induction, unless when subject to a reduced induction regime, which resulted in partial recombination within the intestinal epithelium (Supplementary Fig S5K). We next assessed levels of cell proliferation, migration, apoptosis and linage differentiation in control, *Src KO* and *Src Fyn Yes KO* intestines 4 days after Cre induction.

Figure 5. Src drives ISC hyperproliferation through upregulation of EGFR/MAPK and Stat signalling.

A-D' Immunofluorescence from control (A–B'; *esg^{ts} > gfp*) and Src-overexpressing midguts (C–D'; *esg^{ts} > Src64^{WT}*) stained with anti-pErk1/2 (A, A', C, C'; red or grey) or anti-EGFR (B, B', D, D'; red or grey) after 7 days of transgene expression. *Src* overexpression in ISCs/EBs results in significant upregulation of EGFR and ectopic pErk1/2. Scale bars: 20 μm.

E-F' Magnified views from midguts as in (A, A', C, C'). Note that, while in control midguts pErk1/2 staining is restricted to small nuclei *esg > gfp^{+ve}* cells (E, E'; arrowhead), *esg^{ts} > Src64^{WT}* midguts show ectopic pErk1/2 staining in big nuclei *esg > gfp^{+ve}* cells (F, F'; arrows).

G Quantification of the *esg > gfp/pErk1/2* cell area in midguts as in (E–F'). Data represent mean values ± SEM (***$P < 0.0001$ unpaired *t*-test).

H, I qRT-PCR from whole midguts of genotypes as in (A–D') to measure *degfr* transcript levels (H) and Stat signalling activation thorough *Socs36E* levels (I). *Src* overexpression results in transcriptional upregulation of *egfr* and *Socs36E* in the midgut. Data represent average values ± SEM.

J-M Quantification of ISC proliferation in posterior midguts from animals of the indicated genotypes after 7 days of transgene expression. Knockdown of EGFR/Ras in ISC/EBs suppresses hyperproliferation in Src-overexpressing midguts (J–L). Knockdown of Stat but not the domeless receptor suppresses hyperproliferation in Src-overexpressing midguts (M). Data represent average values ± SEM (***$P < 0.0001$ one-way ANOVA with Bonferroni's multiple comparison test).

Interestingly, intestinal cell proliferation and migration (Supplementary Fig S4A–I) as well as the differentiation of Goblet and enteroendocrine cell lineages (Supplementary Fig S4J–O) were unaffected in *Src Fyn Yes KO* mice. On the other hand, *Src Fyn Yes KO* intestines displayed significant levels of villae apoptosis (Fig 6D–F'' and J) and a complete ablation of Paneth cells (Fig 6G–I and K). No liver phenotypes were detected (Supplementary Fig S5A–K). Consistent with the absence of Paneth cells, which are essential components of the mouse intestinal stem cell niche (Sato *et al*, 2011), isolated crypts from *Src Fyn Yes KO* intestines were unable to form organoids in culture (Sato *et al*, 2009; Fig 6L–P). These data suggest that, in parallel to our observations in the fly midgut, the activity of SFKs (Src, Fyn and Yes) is required for homeostatic self-renewal of the mammalian intestinal epithelium with the three kinases acting redundantly in such context.

Src is required for mouse intestinal regeneration

We next tested whether Src was required for either intestinal regeneration in the mammalian intestine. Our previous work had identified that Wnt/MYC signalling is essential for intestinal regeneration and tumourigenesis downstream of Apc loss, and that this is conserved from mammals to *Drosophila* (Sansom *et al*, 2004; Ashton *et al*, 2010; Cordero *et al*, 2012a,b).

pSrc was upregulated within the crypt membranes of intestines regenerating following DNA damage by gamma irradiation (Fig 7A and B). Conditional deletion of Src from the intestinal epithelium (Fig 7C and D) was sufficient to impair intestinal regeneration as determined by the decreased number of surviving crypts scored 72 h after damage when compared with equally treated control intestines (Fig 7E and F and Supplementary Fig S5M). Surviving *Src KO* crypts were significantly smaller than their control counterparts (Fig 7C and D and Supplementary Fig S5L and M; arrows) but displayed normal Paneth cell numbers (Supplementary Fig S6A–D). Given that available anti-pSrc antibodies cross-react with multiple SFK members, the reduced p-Src staining observed in irradiated *Src KO* intestines (Fig 7D') suggests that Src is responsible for the majority of SFK activity upregulated during intestinal regeneration. Altogether, these results uncover an essential role of epithelial Src driving mouse intestinal regeneration in response to damage.

We next tested whether mechanisms mediating the role of Src in the *Drosophila* midgut were conserved in the mammalian intestine by examining activation of Erk1/2 and Stat3, the closest orthologue of *Drosophila stat92E/marrelle,* in those regenerating *Src KO* intestines, which showed robust gene knockdown (Fig 7D'). We observed that while pErk1/2 and pStat3 strongly stained throughout the regenerating crypts in control intestines (Fig 7H, K, M and N and Supplementary Fig S6F), small regenerating *Src KO* crypts mimicked those from unirradiated control intestines displaying only a few cells positive for either protein (Fig 7G, J, I, L, M and N and Supplementary Fig S6E and G). Taken together, these results suggest that activation of EGFR/MAPK/Erk and Stat3 signalling is likely to be conserved outcomes downstream of Src activation in the intestine.

Src is required for mouse intestinal tumourigenesis following Apc loss

Finally, we addressed whether Src was important for intestinal tumourigenesis following *Apc* loss in the mouse. We therefore bred *Src$^{fl/fl}$* animals into two models of intestinal tumourigenesis driven by *Apc* loss: the *Apc$^{Min/+}$* and *Lgr5Cre^{ER} Apc$^{fl/fl}$* mice. Both of these models mimic intestinal tumourigenesis; however, the timing of *Src* deletion is different. The *Apc$^{Min/+}$* mouse, which forms adenomas sporadically on loss of the remaining copy of *Apc*, was bred into the *AhCre Src$^{fl/fl}$* mice, and Cre was induced post-weaning. The *Lgr5Cre^{ER} Apc$^{fl/fl}$* mice, which form tumours rapidly following Cre induction (Barker *et al*, 2009), were interbred with *Src$^{fl/fl}$* mice and Cre induction therefore leads to simultaneous loss of *Apc* and *Src*.

Conditional deletion of *Src* significantly increased the survival of *Lgr5Cre^{ER}; Apc$^{fl/fl}$* and *Apc$^{Min/+}$* (*Min*) mice (Fig 8A and B, respectively). We next analysed the intestines of mice from the *Min* cohorts, which present discrete and therefore scorable tumours to further characterize the effect of *Src* deletion on pre-established intestinal adenomas. *Min; AhCre Src$^{fl/fl}$* mice exhibited reduced tumour burden when compared with control ones (Fig 8C). Furthermore, even though the overall distribution of tumour types ($n = 40$ *Min*; $n = 25$ *Min; AhCre Src$^{fl/fl}$*) was similar (Fig 8D and Supplementary Fig S7), *Min; AhCre Src$^{fl/fl}$* small, medium and big adenomas displayed significantly reduced proliferation as determined by BrdU staining (Fig 8E–H and Supplementary Fig S7). Unlike during regeneration (Fig 7G–L), pStat3 and pErk1/2 levels do not appear to provide a robust staining pattern within *Apc$^{Min/+}$* tumours (not shown), which precluded further analysis of the effect of Src on such pathways in tumourigenesis. Importantly, our results indicate that preventing Src activity is sufficient to slow down intestinal tumourigenesis in mammals.

Discussion

Using two genetic model systems, our work provides definitive evidence for a conserved functional role for *Src* in intestinal

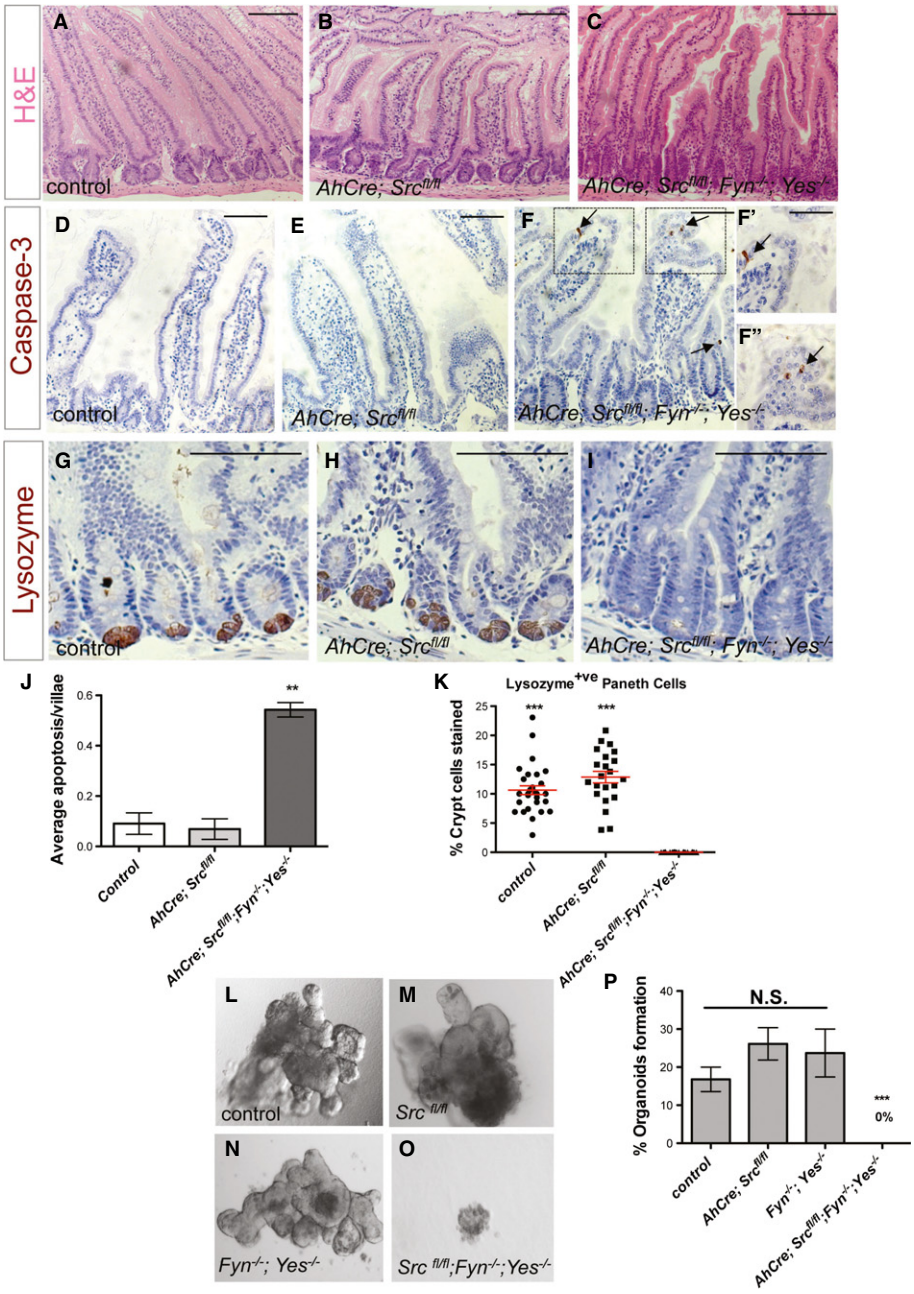

Figure 6. SFKs are redundantly required for mouse intestinal homeostasis.

A–C H&E staining of small intestines from a control mouse (A) or mice subject to 4 days of intestinal epithelial knockout of *Src* only (*AhCre; Src$^{fl/fl}$*) (B) or in combination with constitutive knockout of *Fyn* and *Yes* (*AhCre; Src$^{fl/fl}$; Fyn$^{-/-}$; Yes$^{-/-}$*) (C). Scale bars, 100 μm.

D–I Small intestines from mice as in (A–C) stained with anti-cleaved caspase-3 (D–F") and anti-lysozyme (G–I). Close up views (F', F") from boxed areas in (F). Combined loss of *Src*, *Fyn* and *Yes* leads to villae apoptosis (F–F"; arrows) and loss of Paneth cells (I). Scale bars, 100 μm.

J Quantification of villae apoptosis from intestines as in (D–F). Data represent average values ± SEM (**$P < 0.001$ one-way ANOVA with Bonferroni's multiple comparison test).

K Quantification of the percentage Paneth cells per crypt from intestines as in (G–I). Data represent mean values ± SEM (***$P < 0.0001$ one-way ANOVA with Bonferroni's multiple comparison test).

L–O *In vitro* organoid formation from intestinal crypts of mice of the indicated genotypes. Note that combined loss of *Src*, *Fyn* and *Yes* from the intestinal epithelium prevents organoid formation.

P Quantification of the percentage of organoids formed per 100 crypts seeded. Organoids were scored 1 week after seeding. Data represent average values from two independent experiments ± SEM (***$P < 0.0001$ one-way ANOVA with Bonferroni's multiple comparison test). N.S.: statistically not significant).

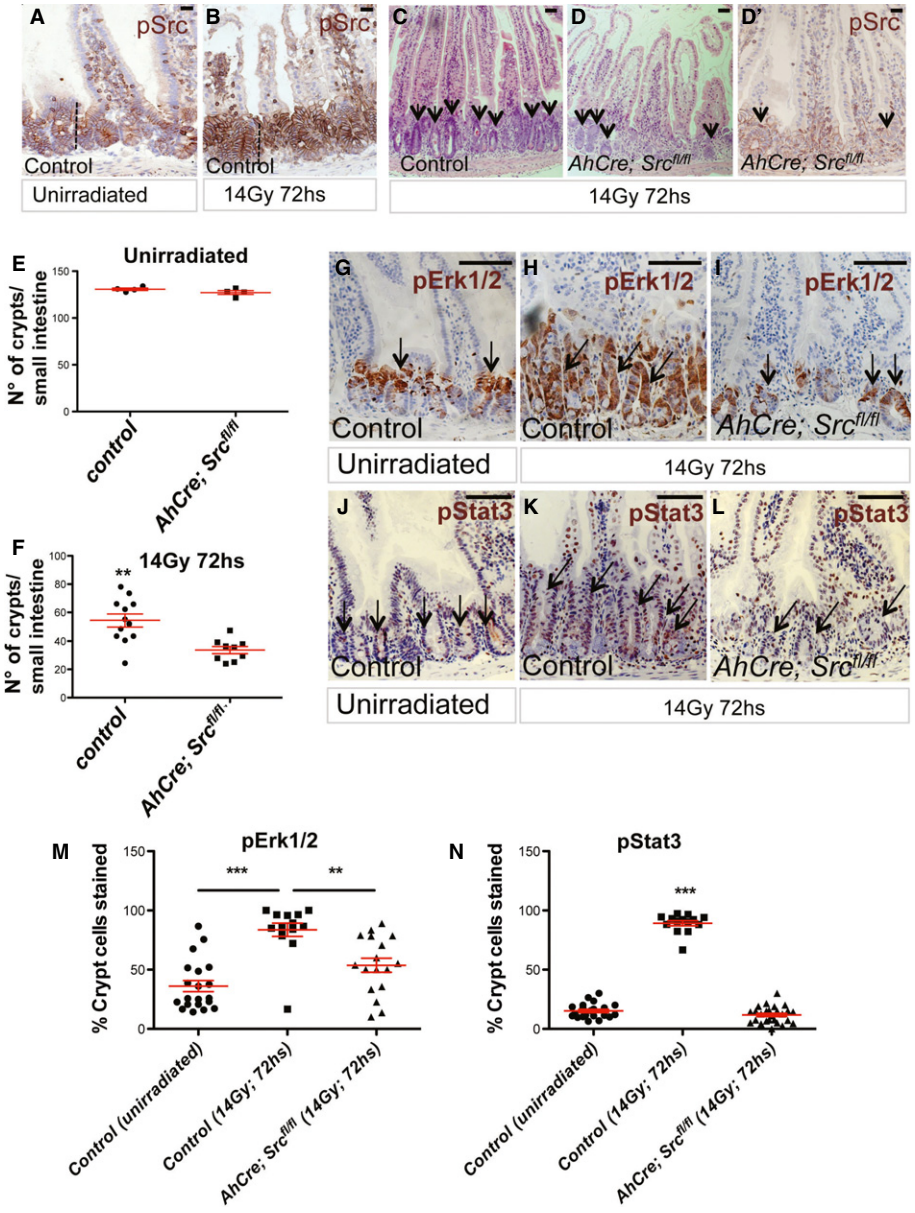

Figure 7. Src is required for mouse intestinal regeneration.

A, B pSrc immunostaining of mouse small intestines from unchallenged control animals or 72 h following DNA damage by gamma irradiation (14 Gy for 72 h). The dotted lines indicate the proliferative crypt domain of the intestine. Scale bars, 200 μm.

C, D H&E staining showing regeneration after DNA damage in the small intestine of a control mouse or following *Src* deletion from the intestinal epithelium (*AhCre; Src*$^{fl/fl}$). Conditional *Src* deletion from the intestinal epithelium resulted in significantly impaired regeneration. pSrc immunostaining of irradiated *AhCre; Src*$^{fl/fl}$ intestines is shown in (D'). Arrows in (C–D') point to regenerating intestinal crypts. Scale bars, 200 μm.

E, F Quantification of the number of crypts in control and *AhCre; Src*$^{fl/fl}$ intestines before and after irradiation. Data are presented as dot plots indicating mean values from all mice scored ± SEM. Each dot represents average value per animal (**P = 0.0016 Unpaired t-test).

G–L pErk1/2 (G–I) and pStat3 (J-L) immunostaining of small intestines from control, unirradiated (G, J), irradiated control (H, K) and *AhCre; Src*$^{fl/fl}$ mice (I, L). Arrows point to regenerating intestinal crypts. Scale bars, 100 μm.

M, N Quantification of the percentage pErk1/2^{+ve} and pStat3^{+ve} cells per crypt from intestines as in (G–L). Data represent mean values ± SEM (***P < 0.0001; **P < 0.001 one-way ANOVA with Bonferroni's multiple comparison test).

regeneration and oncogenic transformation (Fig 9). Moreover, using the adult *Drosophila* intestine, we demonstrate that *Src* is sufficient to drive intestinal hyperproliferation. Our work elucidates a key new role for *Src* during initial stages of tumourigenesis.

A conserved role of SFKs in intestinal stem/progenitor cells

Our results show that Src activation within the mouse intestinal epithelium is restricted to the stem/progenitor cell population,

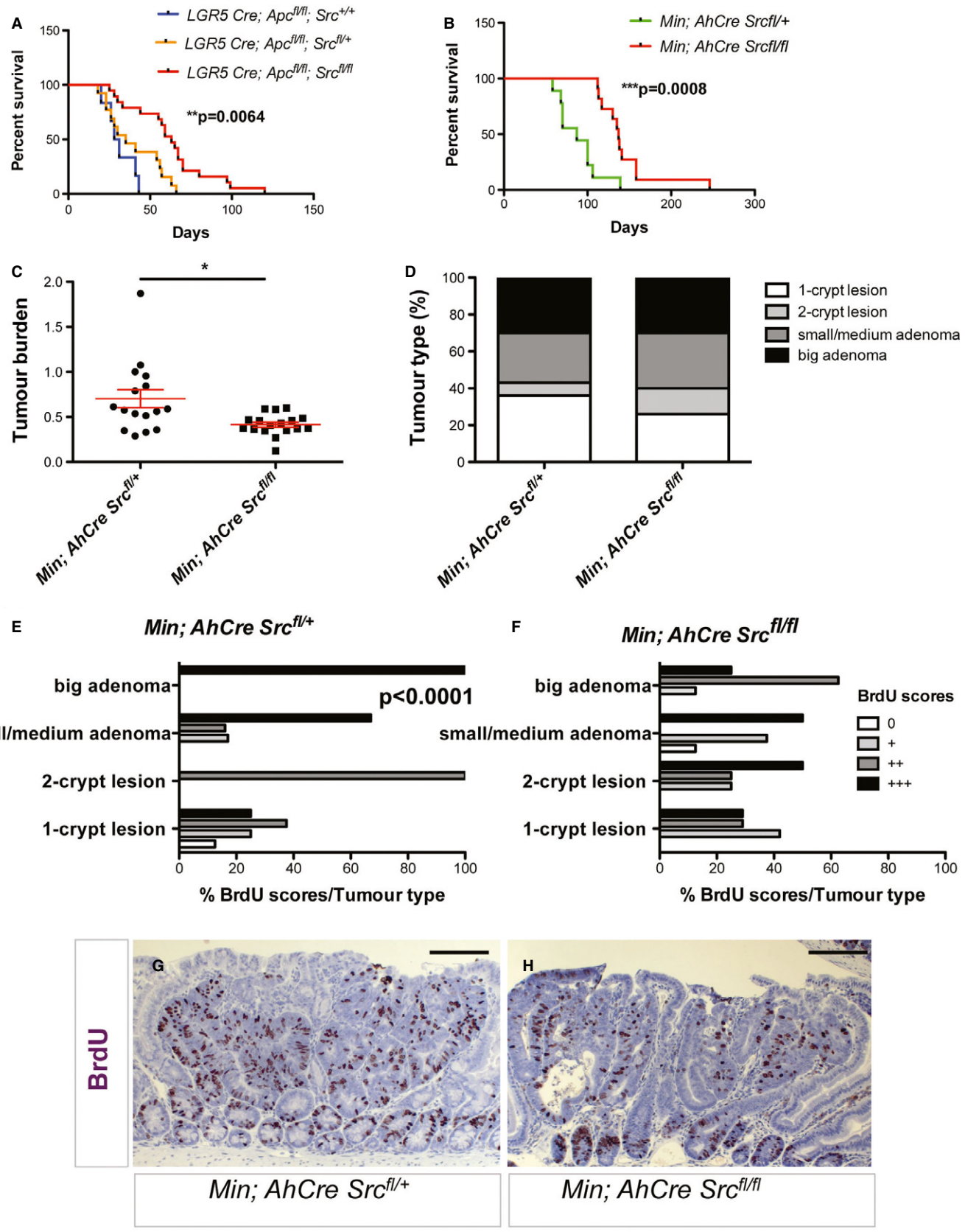

Figure 8. Src is required for Apc-dependent tumourigenesis in the mouse intestine.

A, B Kaplan–Meier survival analysis of animals of the indicated genotypes showed increased survival of animals with combined *Apc* and *Src* deletion in the intestine. *Src* deletion significantly suppressed tumourigenesis in *Lgr5*-Cre^{ER}; *Apc*$^{fl/fl}$ (A) and *Apc*$^{Min/+}$ (B) mouse models of colorectal cancer. The *P*-values of a log-rank test are shown in each panel.

C Intestinal tumour burden (tumour number/tumour area) in *Min; AhCre Src*$^{fl/+}$ (control) and *Min; AhCre Src*$^{fl/fl}$ mice. Data are presented as dot plots indicating mean values from all mice scored ± SEM. Each dot represents average tumour burden per animal (*P = 0.018, unpaired *t*-test).

D Percentage tumour type scored in small intestines from animals as in (C).

E, F BrdU scores from the different tumour types in small intestines from mice as in (C). *Src* deletion from the intestinal epithelium results in reduced proliferation in small/medium and big adenomas from *Apc*$^{Min/+}$ mice (F) (****P < 0.0001, chi-square test).

G, H BrdU immunostaining in big adenomas from mice of the indicated genotypes. Scale bars, 100 μm.

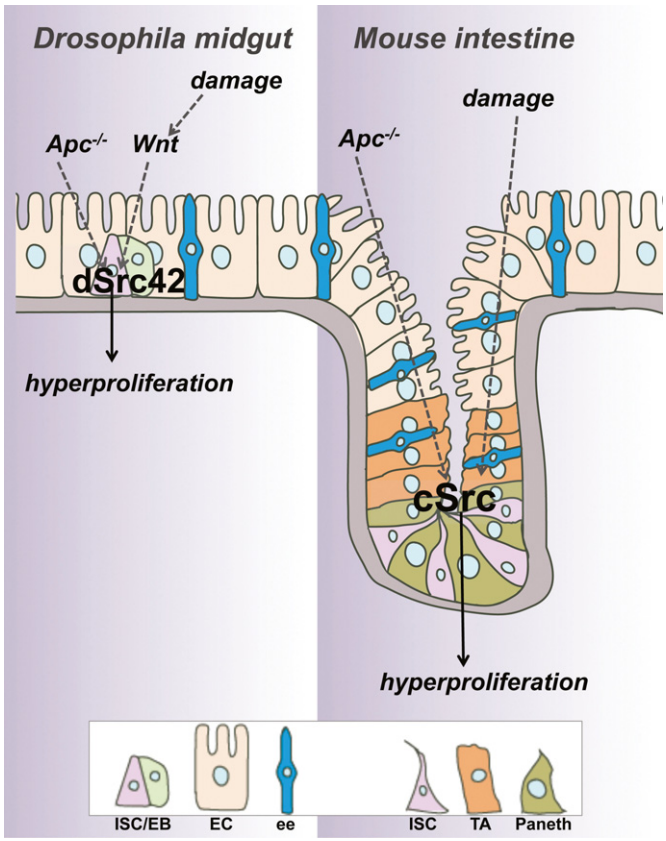

Figure 9. A conserved role of Src in intestinal regeneration and tumourigenesis.

dSrc42/c-Src is activated in response to damage and upon Wg/Wnt signalling upregulation within stem/progenitor cells of the adult *Drosophila* midgut and mouse small intestine leading to tissue hyperproliferation. Src knockdown prevents intestinal regeneration and tumourigenesis in both model systems. ISC/EB: intestinal stem cell/enteroblast; EC: enterocyte; ee: enteroendocrine cell; TA: transit-amplifying cell; Paneth: Paneth cell.

which includes proliferating stem and transit-amplifying cells (Fig 1A). Consistently, functional data on the use of AhCre recombinase demonstrate Src's requirement in intestinal regeneration and *Apc*^{Min}-dependent tumourigenesis. A comparable scenario can be drawn from our studies on the adult *Drosophila* midgut where Src activation is detected and required within the *esg*$^{+ve}$ stem/progenitor cell population represented by ISCs and EBs, respectively (Fig 2–4). Unlike in the mouse intestine, stem cells represent the only proliferative cell within the fly midgut and therefore Src's role can be unambiguously assigned to a function of the protein within stem cells. Similar conclusions are not easy to draw in the mammalian paradigm given the presence of multiple stem cell populations with apparent redundant roles (Tian *et al*, 2011).

Our previous work has shown that Apc deficiency drives a crypt progenitor phenotype, which is mimicked in intestinal regeneration (Sansom *et al*, 2004; Ashton *et al*, 2010). Following *Apc* loss, there is increased stem/progenitor proliferation, perturbed cell migration and a 2–4 increase in Lgr5 positive cells (Sansom *et al*, 2004; Barker *et al*, 2009). These data would suggest that, in order to target Apc-deficient cells, the crypt progenitor phenotype would need to be inhibited and sole inhibition of the Lgr5/stem cell phenotype would not be sufficient. Consistently, recent work has suggested that the Apc crypt progenitor phenotype is not inhibited upon ablation of Lgr5 cells (Metcalfe *et al*, 2014). Thus, our finding that Src is over-expressed within stem and progenitor cells following Apc loss and during regeneration together with Src's requirement in both contexts explains the selectivity of Src for both regenerative and cancer cell proliferation.

Non-redundant roles of SFKs

Work in cell lines has previously shown distinct properties of SFKs (Sandilands *et al*, 2007). However, the evidence regarding non-redundant roles of SFK *in vivo* is rather limited. Examples include classical work on the role of Src in bone formation (Stein *et al*, 1994; Lowell & Soriano, 1996) and recent work indicating a non-redundant role of the kinase in mouse mammary carcinogenesis (Marcotte *et al*, 2012). Our results show that loss of Src is sufficient to slow down intestinal regeneration and tumourigenesis *in vivo* without affecting overall tissue homeostasis. Surprisingly, constitutive loss of Fyn and Yes (*Fyn*$^{-/-}$; *Yes*$^{-/-}$) was also sufficient to prevent intestinal regeneration (Supplementary Fig S5N and O). The overall poor survival of *Fyn*$^{-/-}$; *Yes*$^{-/-}$ mice prevented us from assessing the contribution of those kinases in our intestinal tumourigenesis models. Therefore, there is a therapeutic window, which would allow targeting of Src within transformed intestinal epithelia without affecting the normal tissue.

A redundant role of SFKs in the mammalian intestine

The deletion of Src, Fyn and Yes from the adult intestine using the AhCRE transgene led to ill health so that all mice required euthanasia. *Src Fyn Yes triple KO* intestines displayed two main phenotypes, which were not observed upon loss of Src alone: significant levels of villae apoptosis and ablation of Paneth cells (Fig 6). While the latter is consistent with the inability to obtain intestinal organoids from isolated *Src Fyn Yes KO* crypts, it does not explain animal viability. The precise cause of the ill health is unknown; however, perturbed intestinal epithelial barrier dysfunction, which is in part

characterized by exacerbated villae apoptosis, could cause similar phenotypes. This is currently under further investigation.

Src as a therapeutic target in early stage colorectal tumourigenesis

The complete rescue of Src-dependent hyperproliferation in the fly midgut by human ChK overexpression (Fig 1 and Supplementary Fig S1) suggests a main involvement of Src kinase activity in this process and highlights the level of functional conservation in these kinases. Treatment with the kinase inhibitor dasatinib, a widely used Src inhibitor, has been effective to target Src in multiple cell lines and mouse models of tumour invasion and metastasis (Serrels *et al*, 2006; Morton *et al*, 2010). However, dasatinib and other Src inhibitors have proven ineffective when used in mouse models of CRC initiation (data not shown) as well as in the clinic (Serrels *et al*, 2006). Key issues with such inhibitors are their broad spectrum of targets and unclear *in vivo* efficacy (Brandvold *et al*, 2012). The current scenario emphasizes on the importance of developing more selective Src inhibitors and highlights the need for genetic experiments to validate results from pharmacological targeting of molecules.

Distinct molecular events mediate Src-dependent proliferation in the intestine

Mechanistically, we have defined the action of *Src* in the *Drosophila* intestine as working via EGFR/Erk1/2 and Stat pathway activation (Fig 5). EGFR/Ras activation is a limiting step in stem/progenitor cell proliferation in the fly midgut (Jiang *et al*, 2011). Consequently, our genetic experiments are not sufficient to unambiguously establish the epistatic relationship between Src and EGFR/MAPK signalling. However, our expression data suggest that EGFR levels and pErk activation are increased in response to Src overexpression in the fly midgut. Furthermore, we see impaired activation of Erk1/2 and Stat3 in Src-deficient mammalian intestines during regeneration (Fig 7). Therefore, our evidence suggests that EGFR/MAPK and Stat signalling activation are key events downstream of Src activation in the intestine. However, there may be other pathways downstream of Src aside EGFR/MAPK important for the phenotypes we observed that warrant future testing.

Previous work on *Drosophila* suggests that Src drives hyperproliferation of the developing eye epithelium through parallel activation of Stat and JNK signalling (Read *et al*, 2004). However, such role of Src does not appear to involve EGFR activation. Reciprocally, our results indicate that JNK signalling is, at least not directly, involved in Src-dependent ISC hyperproliferation in the fly midgut. Importantly, our work presents the first direct evidence demonstrating that Wnt signalling is required to activate Src *in vivo* (Fig 3). These results indicate the presence of an 'intestine-specific' molecular network mediating the role of Src in this tissue.

One generic Src target is focal adhesion kinase (FAK). Our previous work in the intestinal epithelium has suggested that this is also a key node for transformation and regeneration (Ashton *et al*, 2010). Therefore, our current results might reflect a regulation of Fak activation by Src. Nevertheless, while our results suggest that Src appears to activate EGFR/Erk1/2 and Stat in the intestine, Fak is primarily required for Akt/mTOR signalling activation in this tissue (Ashton *et al*, 2010). Importantly, unlike *Src*, loss of *Drosophila Fak* (Fox *et al*, 1999; Fujimoto *et al*, 1999; Palmer *et al*, 1999) does not affect intestinal regeneration. Furthermore, *Fak* overexpression in adult *Drosophila* midgut does not lead to ISC hyperproliferation (data not shown). Thus, in contrast to Src, Fak is not sufficient for intestinal hyperproliferation, even though in the mammalian system is necessary for the survival of *Apc*-deficient cells.

In summary, we have elucidated novel roles for Src in intestinal regeneration and as an early driver of tumourigenesis in addition to its established role in invasion and metastasis. Src-overexpressing fly midguts may represent an excellent platform for initial testing of more specific Src inhibitors not yet tested *in vivo* (Brandvold *et al*, 2012). Inhibitors that could specifically target Src may be very useful in those patients that are of high risk of developing CRC.

Materials and Methods

Fly stocks

The following fly stocks were kindly provided to us by our colleagues: the null allele $Apc1^{Q8}$ (Yashi Ahmed), *escargot-gfp* (Shigeo Hayashi), $UAS\text{-}egfr^{DN}$ (Mathew Freeman), $EGFR^{top1}/Cyo$ (Marek Mlodzik), $UAS\text{-}JNK^{DN}$ (Aron DiAntonio), $esg^{ts}F/O$ (Bruce Edgar), *MARCM 82B* line (David Bilder). The rest of the lines used were obtained from VDRC and the Bloomington Stock collection.

VDRC ID numbers

UAS-stat-IR (43866), *UAS-dome-IR* (2612), $UAS\text{-}Src42\text{-}IR^{KK}$ (100708), $UAS\text{-}egfr\text{-}IR^{KK}$ (107130), $UAS\text{-}Ras\text{-}IR^{KK}$ (106642), $UAS\text{-}Ras\text{-}IR^{CG}$ (28129).

Bloomington stock numbers

$UAS\text{-}Src42^{CA}$ (6410), $UAS\text{-}Src64^{wt}$ (8477), $Src42^{K10108}/Cyo$ (10969), $UAS\text{-}Src42\text{-}IR^{CG}$ (44039).

Fly and mouse genetics

A complete list of fly genotypes and mouse strains used in this study can be found as part of the Supplementary Materials and Methods.

Fly maintenance

Crosses were maintained at 18°C in standard medium. Animals of the desired genotypes were collected within 48–72 h of eclosion and then switched to the desired temperature. All experiments involving the activation of a transgene under the control of $gal4/gal80^{ts}$ were switched from 18 to 29°C to allow transgene activation for as long as necessary. Animals were kept in incubators with controlled 12-h light-dark cycles. Flies were changed into new food every 2 days.

Regeneration assays

Experimental flies were collected within 48 h of eclosion at 18°C and moved to 29°C for 14 days on standard media. Flies were then transferred to either 5% sucrose (vehicle) or 10× overnight (*Pe*) culture on filter-paper discs (Whatman) for the last day of the incubation period. Midguts were then dissected and analysed using immunofluorescence and confocal imaging.

Analysis of intestinal homeostasis

Three- to five-day-old animals carrying the inducible 'escargot flip out' system (esg^{ts} *F/O>gfp*; Jiang *et al*, 2009) were switched from 18 to 29°C and their midguts analysed 7, 14 and 30 days after transgene induction to visualize the *esg* cell lineage over time.

Clonal analysis

Recombinant clones were generated using the MARCM technique as previously described (Lee & Luo, 1999). Crosses were carried out at 25°C. Two- to five-day-old adults of the desired genotypes were selected and subject to three 30-min heat shocks at 37°C in 1 day. Flies were then incubated at 25°C for 7, 14 and 30 days.

RNA quantification

Total RNA was extracted from at least 10 midguts using RNAeasy mini kit (Qiagen) followed by DNase treatment (Qiagen). cDNA synthesis was performed using the High-Capacity cDNA reverse transcription kit (Applied Biosystems). Transcript levels were measured using the primers pairs shown underneath. RNA extractions were performed from three biological replicates. DNA was analysed in triplicate using the Applied Biosystems 7500. Expression of the target genes was measured relative to that of *RpL32* (rp49). A series of 10-fold dilutions of an external standard was used in each run to produce a standard curve. MAXIMA SYBR GREEN Master Mix (Fermentas) was used for qPCR following manufacturer's instructions. Data were extracted and analysed using Applied Biosystems 7500 software version 2.0 and Prism GraphPad software. Primer sequences are indicated in Supplementary Table S1.

Sample number and statistical analysis for mouse data

Only posterior midguts of female flies were analysed in this study. Between 7 and 15 midguts were analysed in each experiment. Data were plotted using GraphPad Prism 5 software. Statistical methods used for the analysis of each experiment are detailed in the corresponding figure legends.

Quantification of pErk1/2 and Delta staining

pErk1/2 staining (Fig 5G) was quantified with ImageJ by measuring total esg>gfp^{+ve} and pErk1/2^{+ve} areas normalized by the total number of cells (identified by Dapi staining) within that area. Five posterior midguts were scored per genotype.

The number of ISCs (Fig 1M–P) was scored manually by counting the total number of Delta^{+ve} within a consistent region of the posterior midgut, which was imaged with a 40× objective and comprised a field of 0.04 mm^2. Six to seven posterior midguts were analysed per genotype.

Mouse experiments

All experiments were performed under the UK Home Office guidelines. Mouse strains were backcrossed into a C57Bl6J background for 5–10 generations.

Mice carrying the *AhCre* recombinase were induced by single injection (Supplementary Fig S5K) or 3 daily intraperitoneal (i.p.) injection of 80 mg/kg β-Napthoflavone for 1 day. Intestinal phenotypes were analysed 4, 6 or 7 days after transgene induction. Mice carrying the *Lgr5-CreER* recombinase were given one i.p. injection of 120 mg/kg tamoxifen, followed by one daily i.p. injection of 80 mg/kg tamoxifen for 3 days.

Intestinal regeneration was induced by irradiating mice with 14 Gy gamma irradiation 4 days after recombinase induction. Mice were sacrificed 72 h post-irradiation and the small intestine isolated and flushed with tap water. 10 × 1 cm portions of small intestine were bound together with surgical tape and fixed in 4% neutral buffered formalin. Haematoxylin-and-Eosin-stained sections were used for analysis. Crypts were scored as regenerating if they contained six or more consecutive cells. The average number of regenerating crypts across cross sections of the 10 gut pieces was used for statistical analysis. Intestines from 12 control and nine $Src^{fl/fl}$ mice were analysed. Age-matched (7-day post-induction) unirradiated mice where used as controls (Fig 7E).

Quantification of villae apoptosis

Villae apoptosis was scored by counting the number of cells stained for activated caspase-3 from small intestinal gut rolls.

Quantification of tissue staining

Staining with anti-lysozyme, anti-pErk1/2 and anti-pStat3 was quantified by scoring the percentage of crypt cells, which stained with each of the markers.

Organoid formation assay

Data were scored as the percentage of crypts that formed intestinal organoids in culture 1 week after seeding.

Sample number and statistical analysis for mouse data

In all cases, data represent average values ± SEM from at least three mice. Cell migration values for *AhCre;* $Src^{fl/fl}$*;* $Fyn^{-/-}$*;* $Yes^{-/-}$ mice (Supplementary Fig S4I) are from a single mouse due to the low availability of surviving mice from such genotype.

Data were plotted using GraphPad Prism 5 software. Statistical methods used for the analysis of each experiment are detailed in the corresponding figure legends.

Histology and tissue analysis

Immunofluorescence

Tissues were dissected in PBS and fixed 30 min in 4% paraformaldehyde (Polysciences, Inc.). Midguts processed for pErk1/2 staining were subject to additional fixation in ethanol. After fixation, samples were washed three times in PBS + 0.1% Triton X-100 (PBST) and incubated in primary antibodies overnight at 4°C. Samples were then washed as described and subjected to secondary antibody staining for 2 h at room temperature followed by washing and mounting on Vectashield containing DAPI (Vector Laboratories, Inc.). Primary and secondary antibodies were incubated in PBST+ 0.5% BSA.

*Primary antibodies used (*Drosophila*)*
Chicken anti-GFP 1:4,000 (ab13970; Abcam); mouse anti-dEGFR 1:10 (C-273; Sigma); rabbit anti-pH3 S10 and S28 1:100 (9701 and 9713; Cell Signalling); rabbit anti-p-Src 1:100 (44660G; Invitrogen); rabbit anti-pErk1/2 1:100 (9101; Cell Signalling).

*Secondary antibodies used (*Drosophila*)*
Alexa 488 1:200 and Alexa 594 1:100 (Invitrogen). Nuclei were counterstained with DAPI. Confocal images were collected using a Zeiss 710 confocal microscope and processed with Adobe Photoshop CS.

BrdU labelling
300 μg/ml BrdU (RPN 201V1; GE Healthcare) was mixed into the fly food, and animals were fed *ad libitum* ON prior to midgut dissection. Mouse intestines were labelled by i.p. injection of 250 μl BrdU 2 and 48 h prior to tissue dissection.

Immunohistochemistry of fly midguts
Whole midguts were dissected and fixed at 4°C ON using a 10% formalin solution including 2% toluidine blue to improve visualization of the midguts during the embedding and sectioning process. Tissues were then mounted between two layers of 1% agar with the posterior midguts appropriately oriented. Agar-embedded tissues were further incubated in 10% formalin ON and then subjected to paraffin embedding. The paraffin blocks were trimmed in at 10 μm until the beginnings of the orientated midguts were revealed. Serial 4-μm sections of posterior midguts were cut, placed onto polysine slides and processed for staining.

Immunohistochemistry of mouse intestines
Briefly, tissues were flushed with water and fixed in 4% neutral buffered formalin and then subjected to paraffin embedding and processing for histological analysis.

Primary antibodies used (Mouse tissue)
rabbit anti-p-Src 1:100 (2101; Cell Signalling); rabbit anti-pErk1/2 1:400 (9101; Cell Signalling); rabbit anti-pStat3 1:50 (9131; Cell Signalling); mouse anti-BrdU 1:200 (347580; BD Biosciences); rabbit anti-cleaved caspase-3 1:50 (9661; Cell Signalling); rabbit anti-Ki67 1:100 (RM-9106, Thermo); rabbit anti-lysozyme 1:150 (A099, Dako).

Tissue dyes used
Alcian Blue, Grimelius and Sirius Red staining solutions were used to visualize Goblet and enteroendocrine cells in the intestine and liver fibrosis, respectively.

Secondary antibodies used (Mouse tissue)
Mouse and rabbit EnVision (K4001 and K4003; Dako). Images were collected using an Olympus BX51 microscope and images taken with a DP70 camera and processed with Adobe Photoshop CS.

Supplementary information for this article is available online:
http://emboj.embopress.org

Acknowledgements
We thank all our colleagues, the VDRC and Bloomington stock centres and the Developmental Studies Hybridoma Bank for providing fly lines and reagents. We thank J. Neumann and A. Jung for providing samples from human intestinal adenomas. Julia Cordero would like to thank Rhoda K. Stefanatos for her help with statistical analysis and tutorial on the use of Adobe Illustrator while designing the working model. M.V. and O.J.S. are Cancer Research U.K. investigators. This work was partly funded by a NC3Rs grant. J.B.C has been funded by Marie Curie and EMBO fellowships. J.B.C is a Dorothy Hodgkin Royal Society Fellow and a Glasgow University Leadership Fellow.

Author contributions
JBC designed, performed and analysed experiments and wrote the manuscript. RAR performed and analysed experiments. NV contributed to the analysis of mouse tumours. CN performed immunohistochemistry. MCF analysed experiments and wrote the manuscript. WJM provided $Src^{fl/fl}$ mice and analysed experiments. MV and OJS designed and analysed experiments and wrote the manuscript.

Conflict of interest
The authors declare that they have no conflict of interest.

References

Ahmed Y, Hayashi S, Levine A, Wieschaus E (1998) Regulation of armadillo by a *Drosophila* APC inhibits neuronal apoptosis during retinal development. *Cell* 93: 1171 – 1182

Amcheslavsky A, Jiang J, Ip YT (2009) Tissue damage-induced intestinal stem cell division in *Drosophila*. *Cell Stem Cell* 4: 49 – 61

Andreu P, Colnot S, Godard C, Gad S, Chafey P, Niwa-Kawakita M, Laurent-Puig P, Kahn A, Robine S, Perret C, Romagnolo B (2005) Crypt-restricted proliferation and commitment to the Paneth cell lineage following Apc loss in the mouse intestine. *Development* 132: 1443 – 1451

Ashton GH, Morton JP, Myant K, Phesse TJ, Ridgway RA, Marsh V, Wilkins JA, Athineos D, Muncan V, Kemp R, Neufeld K, Clevers H, Brunton V, Winton DJ, Wang X, Sears RC, Clarke AR, Frame MC, Sansom OJ (2010) Focal adhesion kinase is required for intestinal regeneration and tumorigenesis downstream of Wnt/c-Myc signaling. *Dev Cell* 19: 259 – 269

Barker N, Ridgway RA, van Es JH, van de Wetering M, Begthel H, van den Born M, Danenberg E, Clarke AR, Sansom OJ, Clevers H (2009) Crypt stem cells as the cells-of-origin of intestinal cancer. *Nature* 457: 608 – 611

Beebe K, Lee WC, Micchelli CA (2010) JAK/STAT signaling coordinates stem cell proliferation and multilineage differentiation in the *Drosophila* intestinal stem cell lineage. *Dev Biol* 338: 28 – 37

Biteau B, Jasper H (2011) EGF signaling regulates the proliferation of intestinal stem cells in *Drosophila*. *Development* 138: 1045 – 1055

Biteau B, Hochmuth CE, Jasper H (2011) Maintaining tissue homeostasis: dynamic control of somatic stem cell activity. *Cell Stem Cell* 9: 402 – 411

Brandvold KR, Steffey ME, Fox CC, Soellner MB (2012) Development of a highly selective c-Src kinase inhibitor. *ACS Chem Biol* 7: 1393 – 1398

Buchon N, Broderick NA, Chakrabarti S, Lemaitre B (2009) Invasive and indigenous microbiota impact intestinal stem cell activity through multiple pathways in *Drosophila*. *Genes Dev* 23: 2333 – 2344

Cao X, Tay A, Guy GR, Tan YH (1996) Activation and association of Stat3 with Src in v-Src-transformed cell lines. *Mol Cell Biol* 16: 1595 – 1603

Casali A, Batlle E (2009) Intestinal stem cells in mammals and *Drosophila*. *Cell Stem Cell* 4: 124 – 127

Cordero J, Vidal M, Sansom O (2009) APC as a master regulator of intestinal homeostasis and transformation: from flies to vertebrates. *Cell Cycle* 8: 2926 – 2931

Cordero JB, Sansom OJ (2012) Wnt signalling and its role in stem cell-driven intestinal regeneration and hyperplasia. *Acta Physiol (Oxf)* 204: 137 – 143

Cordero JB, Stefanatos RK, Myant K, Vidal M, Sansom OJ (2012a) Non-autonomous crosstalk between the Jak/Stat and Egfr pathways mediates Apc1-driven intestinal stem cell hyperplasia in the *Drosophila* adult midgut. *Development* 139: 4524 – 4535

Cordero JB, Stefanatos RK, Scopelliti A, Vidal M, Sansom OJ (2012b) Inducible progenitor-derived Wingless regulates adult midgut regeneration in *Drosophila*. *EMBO J* 31: 3901 – 3917

Fox GL, Rebay I, Hynes RO (1999) Expression of DFak56, a *Drosophila* homolog of vertebrate focal adhesion kinase, supports a role in cell migration *in vivo*. *Proc Natl Acad Sci U S A* 96: 14978 – 14983

Fujimoto J, Sawamoto K, Okabe M, Takagi Y, Tezuka T, Yoshikawa S, Ryo H, Okano H, Yamamoto T (1999) Cloning and characterization of Dfak56, a homolog of focal adhesion kinase, in *Drosophila melanogaster*. *J Biol Chem* 274: 29196 – 29201

Irby RB, Mao W, Coppola D, Kang J, Loubeau JM, Trudeau W, Karl R, Fujita DJ, Jove R, Yeatman TJ (1999) Activating SRC mutation in a subset of advanced human colon cancers. *Nat Genet* 21: 187 – 190

Irby RB, Yeatman TJ (2000) Role of Src expression and activation in human cancer. *Oncogene* 19: 5636 – 5642

Ireland H, Kemp R, Houghton C, Howard L, Clarke A, Sansom O, Winton D (2004) Inducible Cre-mediated control of gene expression in the murine gastrointestinal tract: effect of loss of beta-catenin. *Gastroenterology* 126: 1236 – 1246

Jiang H, Patel PH, Kohlmaier A, Grenley MO, McEwen DG, Edgar BA (2009) Cytokine/Jak/Stat signaling mediates regeneration and homeostasis in the *Drosophila* midgut. *Cell* 137: 1343 – 1355

Jiang H, Grenley MO, Bravo MJ, Blumhagen RZ, Edgar BA (2011) EGFR/Ras/MAPK signaling mediates adult midgut epithelial homeostasis and regeneration in *Drosophila*. *Cell Stem Cell* 8: 84 – 95

Jiang H, Edgar BA (2012) Intestinal stem cell function in *Drosophila* and mice. *Curr Opin Genet Dev* 22: 354 – 360

Jones RJ, Avizienyte E, Wyke AW, Owens DW, Brunton VG, Frame MC (2002) Elevated c-Src is linked to altered cell-matrix adhesion rather than proliferation in KM12C human colorectal cancer cells. *Br J Cancer* 87: 1128 – 1135

Kajita M, Hogan C, Harris AR, Dupre-Crochet S, Itasaki N, Kawakami K, Charras G, Tada M, Fujita Y (2010) Interaction with surrounding normal epithelial cells influences signalling pathways and behaviour of Src-transformed cells. *J Cell Sci* 123: 171 – 180

Kinzler KW, Nilbert MC, Su LK, Vogelstein B, Bryan TM, Levy DB, Smith KJ, Preisinger AC, Hedge P, McKechnie D *et al* (1991) Identification of FAP locus genes from chromosome 5q21. *Science* 253: 661 – 665

Korinek V, Barker N, Morin PJ, van Wichen D, de Weger R, Kinzler KW, Vogelstein B, Clevers H (1997) Constitutive transcriptional activation by a beta-catenin-Tcf complex in APC-/- colon carcinoma. *Science* 275: 1784 – 1787

Lee T, Luo L (1999) Mosaic analysis with a repressible cell marker for studies of gene function in neuronal morphogenesis. *Neuron* 22: 451 – 461

Lee WC, Beebe K, Sudmeier L, Micchelli CA (2009) Adenomatous polyposis coli regulates *Drosophila* intestinal stem cell proliferation. *Development* 136: 2255 – 2264

Lin G, Xu N, Xi R (2008) Paracrine Wingless signalling controls self-renewal of *Drosophila* intestinal stem cells. *Nature* 455: 1119 – 1123

Lowell CA, Soriano P (1996) Knockouts of Src-family kinases: stiff bones, wimpy T cells, and bad memories. *Genes Dev* 10: 1845 – 1857

Marcotte R, Smith HW, Sanguin-Gendreau V, McDonough RV, Muller WJ (2012) Mammary epithelial-specific disruption of c-Src impairs cell cycle progression and tumorigenesis. *Proc Natl Acad Sci U S A* 109: 2808 – 2813

Metcalfe C, Kljavin NM, Ybarra R, de Sauvage FJ (2014) Lgr5(+) stem cells are indispensable for radiation-induced intestinal regeneration. *Cell Stem Cell* 14: 149 – 159

Micchelli CA, Perrimon N (2006) Evidence that stem cells reside in the adult *Drosophila* midgut epithelium. *Nature* 439: 475 – 479

Morton JP, Karim SA, Graham K, Timpson P, Jamieson N, Athineos D, Doyle B, McKay C, Heung MY, Oien KA, Frame MC, Evans TR, Sansom OJ, Brunton VG (2010) Dasatinib inhibits the development of metastases in a mouse model of pancreatic ductal adenocarcinoma. *Gastroenterology* 139: 292 – 303

Ohlstein B, Spradling A (2006) The adult *Drosophila* posterior midgut is maintained by pluripotent stem cells. *Nature* 439: 470 – 474

Palmer RH, Fessler LI, Edeen PT, Madigan SJ, McKeown M, Hunter T (1999) DFak56 is a novel *Drosophila melanogaster* focal adhesion kinase. *J Biol Chem* 274: 35621 – 35629

Read RD, Bach EA, Cagan RL (2004) *Drosophila* C-terminal Src kinase negatively regulates organ growth and cell proliferation through inhibition of the Src, Jun N-terminal kinase, and STAT pathways. *Mol Cell Biol* 24: 6676 – 6689

Reed KR, Athineos D, Meniel VS, Wilkins JA, Ridgway RA, Burke ZD, Muncan V, Clarke AR, Sansom OJ (2008) B-catenin deficiency, but not Myc deletion, suppresses the immediate phenotypes of APC loss in the liver. *Proc Natl Acad Sci U S A* 105: 18919 – 18923

Sandilands E, Brunton VG, Frame MC (2007) The membrane targeting and spatial activation of Src, Yes and Fyn is influenced by palmitoylation and distinct RhoB/RhoD endosome requirements. *J Cell Sci* 120: 2555 – 2564

Sansom OJ, Reed KR, Hayes AJ, Ireland H, Brinkmann H, Newton IP, Batlle E, Simon-Assmann P, Clevers H, Nathke IS, Clarke AR, Winton DJ (2004) Loss of Apc *in vivo* immediately perturbs Wnt signaling, differentiation, and migration. *Genes Dev* 18: 1385 – 1390

Sansom OJ, Meniel VS, Muncan V, Phesse TJ, Wilkins JA, Reed KR, Vass JK, Athineos D, Clevers H, Clarke AR (2007) Myc deletion rescues Apc deficiency in the small intestine. *Nature* 446: 676 – 679

Sato T, Vries RG, Snippert HJ, van de Wetering M, Barker N, Stange DE, van Es JH, Abo A, Kujala P, Peters PJ, Clevers H (2009) Single Lgr5 stem cells build crypt-villus structures *in vitro* without a mesenchymal niche. *Nature* 459: 262 – 265

Sato T, van Es JH, Snippert HJ, Stange DE, Vries RG, van den Born M, Barker N, Shroyer NF, van de Wetering M, Clevers H (2011) Paneth cells constitute the niche for Lgr5 stem cells in intestinal crypts. *Nature* 469: 415 – 418

Sauer B (1998) Inducible gene targeting in mice using the Cre/lox system. *Methods* 14: 381 – 392

Serrels A, Macpherson IR, Evans TR, Lee FY, Clark EA, Sansom OJ, Ashton GH, Frame MC, Brunton VG (2006) Identification of potential biomarkers for measuring inhibition of Src kinase activity in colon cancer cells following treatment with dasatinib. *Mol Cancer Ther* 5: 3014 – 3022

Seton-Rogers S (2013) Colorectal cancer: a powerful model. *Nat Rev Cancer* 13: 8 – 9

Stein PL, Vogel H, Soriano P (1994) Combined deficiencies of Src, Fyn, and Yes tyrosine kinases in mutant mice. *Genes Dev* 8: 1999 – 2007

Talamonti MS, Roh MS, Curley SA, Gallick GE (1993) Increase in activity and level of pp60c-src in progressive stages of human colorectal cancer. *J Clin Invest* 91: 53 – 60

Termuhlen PM, Curley SA, Talamonti MS, Saboorian MH, Gallick GE (1993) Site-specific differences in pp60c-src activity in human colorectal metastases. *J Surg Res* 54: 293 – 298

The Cancer Genome Atlas Network (2012) Comprehensive molecular characterization of human colon and rectal cancer. *Nature* 487: 330 – 337

Tian H, Biehs B, Warming S, Leong KG, Rangell L, Klein OD, de Sauvage FJ (2011) A reserve stem cell population in small intestine renders Lgr5-positive cells dispensable. *Nature* 478: 255 – 259

Vidal M, Larson DE, Cagan RL (2006) Csk-deficient boundary cells are eliminated from normal *Drosophila* epithelia by exclusion, migration, and apoptosis. *Dev Cell* 10: 33 – 44

Vidal M, Warner S, Read R, Cagan RL (2007) Differing Src signaling levels have distinct outcomes in *Drosophila*. *Cancer Res* 67: 10278 – 10285

Yeatman TJ (2004) A renaissance for SRC. *Nat Rev Cancer* 4: 470 – 480

Yu CL, Meyer DJ, Campbell GS, Larner AC, Carter-Su C, Schwartz J, Jove R (1995) Enhanced DNA-binding activity of a Stat3-related protein in cells transformed by the Src oncoprotein. *Science* 269: 81 – 83